Size and locomotor ecology have differing effects on the external and internal morphologies of squirrel (Rodentia: Sciuridae) limb bones

Short title: squirrel limb bone evolution

Authors: Johannah Rickman[1*], Abigail E. Burtner[1*], Tate J. Linden[1], Sharlene E. Santana[1], & Chris J. Law[1,2,3*]

[1]Department of Biology and Burke Museum of Natural History and Culture, University of Washington, Seattle WA 98105; [2]Department of Integrative Biology, University of Texas, Austin, TX; [3]Department of Mammalogy, American Museum of Natural History, New York, NY

*contributed equally

Key words: bone structure, ecomorphology, evolutionary allometry, femur, geometric morphometrics, humerus

Abstract

Mammals exhibit a diverse range of limb morphologies that are associated with different locomotor ecologies and structural mechanics. Biologists, however, have rarely investigated whether these factors have different effects on the external and internal morphologies of limb bones. Here, we used squirrels (Sciuridae) as a model clade to examine the effects of locomotor mode and allometry on the size, external shape, and internal structure of the two major limb bones, the humerus and femur. We quantified these humeral and femoral traits using 3D geometric morphometrics and bone structure analyses on a sample of 76 squirrel species across

their four major ecotypes. We found significant allometric patterns among squirrel ecotypes in the internal structures of humeri and femora but not in their external shapes. Although humeral and femoral external shape statistically differ among squirrel ecotypes, these associations are lost when analyses account for phylogenetic relationships among species. That all ecotypes are phylogenetically clustered suggests humeral and femoral shape variation partitioned early between clades and their ecomorphologies were maintained to the present. In contrast, interactions between size and ecotype predict variation of the internal structures of these long bones after accounting for phylogenetic relationships. The humeri and femora of ground and tree squirrels tend to exhibit increased bone compactness and more robust diaphyses with increasing bone size, adaptations that would facilitate more efficient digging behaviors. Conversely, there were no allometric changes in internal bone structure of gliding squirrels possibly due to constraints for gliding. Lastly, we found that the external shape of the limbs was associated with changes in cross-sectional shape and diaphysis elongation but not with global bone compactness. Overall, these results indicate that mechanical constraints, locomotor ecology, and evolutionary history may enact different pressures on the external and internal morphology of limb bones in mammals.

Introduction

Mammals exhibit a variety of locomotor modes to transverse across a wide range of habitats (Hildebrand 1985). Adaptations to these various locomotor modes are repeatedly observed in mammalian limbs (Polly 2007). For example, scansorial mammals tend to exhibit more elongate, gracile limb bones (Alexander et al. 1979; Burr et al. 1989; Kimura 1991; Polly 2007), whereas fossorial mammals exhibit relatively shorter and more robust limb bones in

response to stress enacted on the bone when digging (Peterka 1936; Gasc et al. 1985; Straehl et al. 2013; Montoya-Sanhueza and Chinsamy 2017). Furthermore, different locomotor modes used in varying environments necessitate long bones being able to resist possible deformation to locomotion-specific forces. For example, species that glide or leap exhibit long limbs and relatively small bodies with barrel-shaped femora potentially in response to the high-takeoff and landing forces (Burr et al. 1989; Hunt et al. 2021). In contrast, highly fossorial mammals exhibit large amounts of compact cancellous bone in the forelimb that exceeds the amount typically seen in most other subterranean mammals (Amson et al. 2022).

The morphology of limb bones is also influenced by body size (Alexander et al. 1979; Biewener 1983; Christiansen 1999; Amson and Bibi 2021). As body size increases, more mechanical support is needed to compensate for an increase in the mechanical forces exerted during locomotion (McMahon 1973; Biewener 1990; Christiansen 1999), which may result in adaptations in the external shape and/or internal structure of the limb bones. Increasing body size is associated with increasing bone robustness in multiple lineages of tetrapods (Alexander et al. 1979; Demes and Jungers 1993; Christiansen 1999; Doube et al. 2009; Ryan and Shaw 2013; Mielke et al. 2018). In quadrupedal terrestrial tetrapods, body size rather than locomotor mode has a stronger influence on conserved limb bone traits such as the minor diaphyseal circumference of weight-bearing bones and the ratio between the stylopodial circumference and body mass (Campione and Evans 2012). Body size may also impose limits on external bone shape; some cursorial carnivorans without the ability to supinate their forelimbs appear to have a smaller maximum body size, while carnivorans with more generalized bone shapes exist at much larger body sizes (McMahon 1973; Polly 2007; Fabre et al. 2015).

While the influence of body size on external limb bone morphology has been researched extensively, relatively fewer studies have examined bone structural characteristics such as bone compactness, second moment of area, or cross-sectional shape, even though these traits affect the mechanics and locomotor ecologies of species (Amson et al. 2022). Additionally, the interaction between allometry and ecological effects on limb bone morphology has received little attention, despite implications about how different locomotory modes may affect overall limb bone evolution (Hayssen 2008; Wölfer et al. 2019; Linden et al. 2023). The internal structure of bone is highly plastic (Amson et al. 2018) due to the ability of bone tissue to remodel in response to its mechanical environment (i.e., Wolff's Law) (Dawson 1980; Ruff et al. 2006; Meier et al. 2013; Kivell 2016). Specializations that occur within the inner bone structure increase mechanical efficiency in movement and decrease stress on the bone (Scheidt et al. 2019). Acclimatization to the mechanical environment occurs throughout an individual's lifetime, but can also be inherited and therefore occur across generations (Cowin et al. 1992; Ruff et al. 2006). The structure and cross-sectional characteristics of long bones have long been used as a representation of how locomotion-related forces affect the development and evolution of limbs (Currey and Alexander 1985; Schaffler et al. 1985; Burr et al. 1989; Amson et al. 2022). However, there are still many gaps in knowledge regarding the macroevolution of internal bone structures and the extent of whether locomotor ecologies and size have differing effects on the external and internal morphologies of limb bones.

In this study, we used squirrels (Sciuridae) as a model clade to examine the effects of locomotor mode and body size on the size, shape, and internal structure of the humerus and femur. The squirrel family consists of approximately 280 species that inhabit a variety of microhabitats, from far above ground in tree canopies to deep underground in burrow systems.

Squirrel species can be categorized into four ecotypes with distinct locomotor ecologies and behaviors: ground squirrels that dig, tree squirrels that climb, gliding squirrels that glide between trees, and more versatile chipmunks that both dig and climb. Previous work has examined relationships between limb lengths and ecotypes, finding, for example, that gliding squirrels exhibit relatively longer forelimbs than all other ecotypes (Peterka 1936; Bryant 1945; Thorington and Heaney 1981; Grossnickle et al. 2020; Linden et al. 2023) and ground squirrels exhibit relatively shorter forelimbs with increasing body elongation (Linden et al. 2023). Furthermore, across Sciuromorpha (squirrel-like rodents), cross-sectional characteristics (i.e., cross-sectional area and second moment of area) of the femur scale with positive allometry with respect to body mass (Scheidt et al. 2019). Whether the external shape and internal structure of the humerus and femur differ among ecotypes remains to be tested within this clade.

Our objectives were two-fold. First, we examined the scaling relationships of the external shape and internal structure in the humerus and femur. We predicted that both the humerus and femur would be more robust, compact, and exhibit a more oval-shaped cross-section with increasing bone size to resist the relatively greater mechanical forces that occur at larger body sizes (McMahon 1973; Biewener 1990; Christiansen 1999). Second, we tested whether these scaling relationships differ among ecotypes. We predicted that ground squirrels would have more robust, compact limb bones with oval-shaped cross-sections that are needed for force generation during scratch-digging (Hildebrand 1985, 1995; Lagaria and Youlatos 2006). We predicted that chipmunks and tree squirrels would exhibit more generalized limb bone shapes in comparison to other ecotypes as they employ running, climbing, and digging behaviors. Finally, we predicted that gliding squirrels will exhibit more elongate, gracile limb bones with circular-shaped cross-sections to increase patagia surface area for gliding.

Methods

Morphological data

We acquired three-dimensional scans of humeri and femora from 76 squirrel species. through computed tomography (CT) scanning with a Skyscan1172 μCT, Skyscan1173 μCT, GE Phoenix Nanotom M, and NSI X5000 scanning systems. Scans were performed with a resolution of 26.05μm. Scan data was reconstructed using NRecon and then exported and segmented in 3D Slicer (Kikinis et al. 2014). All specimens were sourced from the collections of 11 museums (Table S1). We used female, male, and sex-unknown individuals for our measurements to achieve the largest number of species. We determined that each specimen was fully mature by verifying that the cranial exoccipital-basioccipital and basisphenoid-basioccipital sutures were fused and that all vertebrae and limb bones were ossified.

Ecotype classification

Following Linden et al. (2023), we categorized species into four ecotypes—chipmunk (n = 14), gliding (n = 8), ground (n = 25), or tree (n = 29)—based on either locomotion, evolutionary grouping, or reproductive behavior (Fig. 1). Species that reproduce in underground burrows were categorized as ground, species in genus *Tamias* that spend significant time in trees either during birth or post-birth were categorized as chipmunk, species that reproduce in nests as were categorized tree, and species that have patagia were categorized as gliding.

External shape analyses

All phylogenetic analyses were conducted using a pruned version of the Upham et al. (2019) phylogeny. All statistical analyses were performed in R (2022). We quantified humeral and femoral size and shape using three-dimensional geometric morphometrics (Rohlf and Slice 1990; Zelditch et al. 2012). We first transformed all specimens to correspond to the left side (an arbitrary choice) of the body using the Transforms module in 3D Slicer (Fedorov et al. 2012). We generated 194 pseudolandmarks on a humerus template and 152 pseudolandmarks on a femur template using the PseudoLMGenerator module of the SlicerMorph extension (Rolfe et al. 2021) in 3D Slicer (Fedorov et al. 2012). The most average squirrel in our dataset (determined visually as the Western gray squirrel, *Sciurus griseus*) was used as our template. Following Diamond et al. (in press), we transferred the pseudolandmarks from the template model to each individual humerus and femur 3D model using the ALPACA module (Porto et al. 2021) in SlicerMorph (Fig. 1). We conducted a General Procrustes Analysis (GPA) using the gpagen function in the R package geomorph (Baken et al. 2021; Adams et al. 2022). We then verified that there were no significant shape differences between limb bones originating from the left or right side with Procrustes ANOVAs (humerus: $F = 1.10$, $Z = 0.489$, $p = 0.319$; femur: $F = 1.38$, $Z = 1.03$, $p = 0.156$).

We used humeral and femoral centroid size as our metrics of humeral and femoral size, respectively. We tested if humeral and femoral size differed among ecotypes using a phylogenetic ANOVA with the R package phylolm v2.6.2 (Tung Ho and Ané 2014). To determine if there were significant differences in limb sizes among ecotypes, we generated 95% confidence intervals using bootstrapping with 1000 replications. Differences in limb sizes were

158 considered significant if an ecotype's mean limb size was outside of other ecotypes' 95%
159 bootstrap confidence intervals.
160 We then tested whether humeral and femoral shape allometry differed among ecotypes
161 using Procrustes ANCOVAs and phylogenetic Procrustes ANCOVAs (i.e., limb shape ~ ln limb
162 size * ecotype) with 1000 random residual permutation procedure iterations using the functions
163 procD.lm and procD.pgls with the R package geomorph v4.0.4 (Baken et al. 2021; Adams et al.
164 2022) and post hoc pairwise permutation tests using the function pairwise in RRPP v1.3.1
165 (Collyer et al. 2015; Adams and Collyer 2018). We also tested whether humeral and femoral
166 shape allometry differed within each ecotype using phylogenetic Procrustes regression with 1000
167 random residual permutation procedure iterations. Because there were no significant shape
168 allometries across and among ecotypes (see Results), we tested whether humeral and femoral
169 shape differed among ecotypes using Procrustes ANOVAs and phylogenetic Procrustes
170 ANOVAs (i.e., limb shape ~ ecotype) with 1000 random residual permutation procedure
171 iterations. Because accounting for phylogenetic relationships affects these statistical significance
172 (see Results), we repeated our shape analyses using a phylogenetic penalized-likelihood
173 multivariate analysis of variance (PL-MANOVA) that jointly estimates Pagel's lambda to
174 account for phylogenetic covariations present in the model residuals using the mvgls and
175 manova.gls functions (Clavel et al. 2019; Clavel and Morlon 2020) from the R package
176 mvMORPH v.1.1.6 (Clavel et al. 2015). This approach uses a penalized-likelihood to fit linear
177 models to high-dimensional data sets where the number of variables is much larger than the
178 number of observations (Clavel et al. 2019). We performed the multivariate test using Pillai's
179 trace. We were unable to perform pairwise testing among ecotypes because the mvMORPH
180 function pairwise.glh is only suited for binary data thus far. Lastly we predicted how well

ecotype can predict limb shape using canonical variate analyses (CVA) with a jackknife cross-validation procedure in the R package Morpho (Schlager 2017).

We visualized the phylomorphospace of humeral and femoral shape by performing principal component analyses (PCA) using the gm.prcomp function in geomorph (Baken et al. 2021; Adams et al. 2022). We also visualized differences between PC extremes by creating average shape models using the Morpho package in R (Schlager 2017) and used a custom Python script (Diamond et al. in press) to extract the mesh distances from the areas with pseudolandmark points.

Bone structure analyses

We used Python-based Slicer module SegmentGeometry (Huie et al. 2022) to create slice-by-slice proximodistal profiles of each scanned specimen. Each profile consisted of length (in millimeters), cross-sectional area (in square millimeters), second moment of area around the major principal axis, second moment of area around the minor principal axis, and compactness (ratio between sample cross-sectional area and total cross-sectional area). Outputs from SegmentGeometry were used to calculate three bone structure traits: global compactness (Cg), diaphysis elongation (DE), and cross-sectional shape (CSS). These three traits reflect bending direction, torsion, and compressive loads (Amson and Bibi 2021). Each variable was computed across 40% of the bones' functional length in order to ensure only the diaphysis was measured. Cg was defined as the mean compactness of all included slices, DE was defined as the ratio between the functional length of the bone and the square-root of the cross-sectional area at the midshaft slice, and CSS was defined as the ratio of the second moment of area around the major

203 principal axis to the second moment of area around the minor principal axis at the midshaft slice
204 (Fig. 1).
205 We determined whether ecotype influences the relationship between each bone structure
206 (i.e., Cg, DE, CSS) and bone size using phylogenetic generalized least squares (PGLS) with an
207 ANCOVA design (i.e., bone structure variable ~ ln bone size * ecotype). Regression coefficients
208 were approximated from a phylogenetic signal within the residual error as Pagel's lambda using
209 the R package phylolm v2.6.2 (Tung Ho and Ané 2014). To determine if bone structure
210 allometry was significant, we used bootstrapping with 1000 replications to generate 95%
211 confidence intervals for the slope for each ecotype. Confidence intervals greater than zero were
212 considered to represent positive allometry, while confidence intervals less than zero were
213 considered to represent negative allometry. Confidence intervals that included zero were
214 considered isometric due to the dimensionless quality of the bone structure variables.
215 Allometries between two ecotypes were considered significantly different if the mean slope was
216 outside the confidence interval of the compared ecotype. We determined whether each bone
217 structure variable differed among ecotypes while controlling for bone size using a second PGLS
218 with an ANCOVA design with no interaction term (i.e., bone structure variable ~ ln bone size +
219 ecotype); we removed the interaction term because slopes from the first PGLS model did not
220 differ among ecotypes (see Results). To determine if there were significant differences in bone
221 structure among ecotypes, we used bootstrapping with 1000 replications to generate 95%
222 confidence intervals for the intercept for each ecotype. Relationships between two ecotypes were
223 considered different if the mean intercept was outside the confidence interval of the compared
224 ecotype.

We compared the bone structure variables between the humerus and femur for each ecotype using paired t-tests (alpha = 0.05).

Relationships between external shape and internal structure

We examined if there were significant relationships between the external shape and each internal structure variable of the humerus and femur among ecotypes by using phylogenetic Procrustes ANCOVAs (i.e., external shape ~ bone structure variable * ecotype) with 1000 random residual permutation procedure iterations and post hoc pairwise permutation tests in the R package geomorph version 4.0.4 (Baken et al. 2021; Adams et al. 2022).

Results

Humeral and femoral size

We found significant differences in humeral size among some ecotypes: chipmunks (mean humeral size [95% CI] = 4.6 [3.8:5.3] cm) exhibited smaller humeri than gliding squirrels (5.4 [4.8:6.1] cm) and tree squirrels (5.2 [4.8:5.7] cm) but not ground squirrels (5.0 [4.4:5.6] cm) (Fig. 2A). We also found significant differences in femoral size among some ecotypes: chipmunks (mean femoral size [95% CI] = 4.8 cm [4.0 : 5.5 cm]) exhibited smaller femora than gliding squirrels (5.6 cm [4.9 : 6.3 cm]) and tree squirrels (5.4 [4.9 : 5.8 cm]) but not ground squirrels (5.2 cm [4.6 : 5.9 cm]) (Fig. 2B).

Humeral external shape analyses

We found no significant humeral shape allometry across all squirrels and no differences in allometry among ecotypes using both Procrustes ANCOVA and phylogenetic Procrustes

ANCOVA (Table 1; Fig. 3). Individual ecotypes also did not exhibit significant humeral shape allometry (Table S2). Procrustes ANOVA indicated that there was a significant relationship between humeral shape and ecotype ($R^2 = 0.38$, $Z = 5.69$, $P < 0.001$), and post-hoc pairwise tests revealed that there were significant differences in humeral shape among among all ecotypes (all $P < 0.002$) except between chipmunks and tree squirrels ($P = 0.075$). Accounting for phylogenetic relationships among species also led to different results based on whether phylogenetic signal was jointly estimated. Incorporating phylogenetic signal revealed a significant relationship between humeral shape and ecotype (PL-MANOVA: lambda = 0.178, Pillai's test = 2.823, $P = 0.001$) whereas models assuming full Brownian motion indicated that there was no significant relationship between humeral shape and ecotype (phylogenetic Procrustes ANOVA: $R^2 = 0.04$, $Z = -0.261$, $P = 0.602$). The CVA with jackknife cross-validation reclassified humeral shapes in their correct ecotype with 93.4% accuracy. Among ecotypes, it accurately reclassified 100% of gliding and ground squirrels, 85.7% of chipmunks, and 89.7% of tree squirrels.

PC1 accounted for 36.8% of the humeral shape variation and largely separates the morphospaces among ground squirrels, chipmunks and tree squirrels, and gliding squirrels (Fig. 4). PC1 primarily describes the lengthening of the humerus. Positive PC1 scores are associated with more robust humeri with more pronounced supinator crests, deltoid tuberosities, and medial epicondyles, whereas negative PC1 scores are associated with more elongate humeri with less developed supinator crests, deltoid tuberosities, and medial epicondyles. PC2 accounted for 12.5% of the humeral shape variation and is associated with shape variation at the ends of the humerus (Fig. 4). Positive PC2 scores are associated with shape variation at the medial

epicondyle and negative PC2 scores are associated with changes at the condyle. Much of this variation across PC2 explains within-ecotype differences.

Femoral external shape analyses

Femoral shape allometries differed significantly among ecotypes (Table 1). Gliding and ground squirrels exhibited significant femoral shape allometry but neither chipmunks nor tree squirrels did (Supplementary Table S2). However, when accounting for phylogenetic relationships among species, we found no significant femoral shape allometry across all squirrels, no differences in allometry among ecotypes (Table 1; Fig. 3), and no femoral shape allometry within individual ecotypes (Supplementary Table S2). Procrustes ANOVA indicated that there was a significant relationship between femoral shape and ecotype ($R^2 = 0.31$, $Z = 6.88$, $P < 0.001$), and post-hoc pairwise tests revealed that there were significant differences in humeral shape among among all ecotypes (all $P < 0.004$). However, accounting for phylogenetic relationships among species indicated that there was no significant relationship between femoral shape and ecotype with (PL-MANOVA: lambda = 0.18, Pillai's test = 2.57, $P = 0.219$) and without (phylogenetic Procrustes ANOVA: $R^2 = 0.04$, $Z = -0.446$, $P = 0.676$) jointly estimating phylogenetic signal. The CVA accurately reclassified femoral shapes in their correct ecotype with 90.8% accuracy. It accurately reclassified 100% of gliding squirrels, 96.6% of tree squirrels, 92.9% of chipmunks, and 80.0% of ground squirrels.

PC1 accounted for 29.3% of the femoral shape variation and separated the morphospace of gliding squirrels from a morphospace largely containing ground squirrels, chipmunks, and tree squirrels (Fig. 4). Positive PC1 scores are associated with more robust femora with more pronounced femoral heads, patellar grooves, greater trochanters, third trochanters, and lesser

trochanters whereas negative PC1 scores are associated with more elongate, gracile femora (Fig. 4). PC2 accounted for 12.8% of the femoral variation and loosely separated tree squirrels from ground squirrels and chipmunks. Positive PC2 scores are associated with shape variation around the greater trochanter and one side of the lesser trochanter, whereas negative PC2 scores are associated with shape variation around the femoral head, greater trochanter, and the opposite side of the lesser trochanter (i.e., one extreme reflects shape variation "bending" the trochanter out and the other in dorsal-ventrally) (Fig. 4).

Humeral internal structure analyses

Across all ecotypes, humeral Cg was positively related with humeral centroid size (PGLS: $R^2 = 0.06$, $\lambda = 0.43$, slope [95% CI] = 0.05 [0.00 - 0.10]). Scaling relationships differed among ecotypes (PGLS with ANCOVA design: $R^2 = 0.22$, $\lambda = 0.00$). Tree squirrel (0.12 [0.04 - 0.20]) and ground squirrel (0.08 [0.01 - 0.14]) humeral Cg were significantly positively related with humeral centroid size, which indicates ground and tree squirrels have evolved to have more compact humeri as humeral size increases. In contrast, chipmunk (-0.05 [-0.41:0.34]) and gliding squirrel (0.06 [-0.02:0.14]) humeral Cg were not significantly related with humeral centroid size. There were no significant differences in humeral Cg among ecotypes (PGLS with ANCOVA design: $R^2 = 0.03$, $\lambda = 0.39$; mean humeral Cg [95% CI] for chipmunks = 0.60 [0.50:70], gliding squirrels = 0.62 [0.55:0.71], ground squirrels = 0.67 [0.58:0.75], and tree squirrels = 0.64 [0.59:0.70]; Fig. 6).

There was no relationship between humeral DE and humeral size across all ecotypes (PGLS: $R^2 = 0.08$, $\lambda = 0.77$, slope [95% CI] = -0.06 [-2.08:1.03]), whereas relationships between humeral DE and humeral size differed among ecotypes (PGLS with ANCOVA design: $R^2 =$

316 0.71, $\lambda = 0.00$). Tree squirrel humeral DE was significantly negatively related with centroid size
317 (-2.07 [-3.93:-0.36]), indicating that tree squirrels evolved less elongate humeri as humeral size
318 increases. Chipmunk (0.05 [-6.57:6.63), gliding squirrel (1.42 [-0.61:3.45), and ground squirrel (-
319 1.10 [-2.73:0.47]) humeral DE were not significantly related with humeral centroid size. There
320 was a significant relationship between humeral DE and ecotype (PGLS with ANCOVA design:
321 $R^2 = 0.68$, $\lambda = 0.00$) where gliding squirrels exhibited higher DE values (mean humeral DE
322 [95% CI] = 26.55 [20.77:32.95]) and thus more elongate humeral diaphyses than chipmunks
323 (20.78 [15.81:26.11]), ground squirrels (18.683 [13.30:24.78]), and tree squirrels (20.89
324 [15.46:26.97]; Fig. 6).
325 Humeral CSS was positively related with humeral centroid size across all ecotypes
326 (PGLS: $R^2 = 0.21$, $\lambda = 0.38$, slope [95% CI] = 0.28 [0.08 - 0.47]). Scaling relationships differed
327 among ecotypes (PGLS with an ANCOVA design: $R^2 = 0.42$, $\lambda = 0.00$). Ground squirrel humeral
328 CSS was significantly positively related with humeral centroid size (0.42 [0.18 - 0.64]), which
329 indicates that ground squirrels evolved more oval-shaped humeral cross-sections as humeral size
330 increases. There was no significant relationship between humeral CSS and humeral size in either
331 chipmunks (0.37 [-0.64:1.46]), gliding squirrels (0.02 [-0.32:0.38]), or tree squirrels (0.21 [-
332 0.08:0.49]). There were also no significant differences in humeral CSS among the ecotypes when
333 accounting for size (PGLS with an ANCOVA design: $R^2 = 0.40$, $\lambda = 0.00$; mean humeral CSS
334 [95% CI] for chipmunks = 0.10 [-0.66:0.90], gliding squirrels = -0.14 [-1.06:0.80]), ground
335 squirrels = 0.41 [-0.44:1.27], and tree squirrels = 0.12 [-0.72:1.00]; Fig. 6).
336

Femoral internal structure analyses

Across all ecotypes, femoral Cg was positively related with femoral size (PGLS: R^2 = 0.17, λ = 0.25, slope [95% CI] = 0.08 [0.03 - 0.13]). Scaling relationships differed among ecotypes (PGLS with an ANCOVA design: R^2 = 0.28, λ = 0.00). Tree squirrel (0.12 [0.04 - 0.20]) and ground squirrel (0.08 [0.01 - 0.14]) femoral Cg were significantly positively related with femoral size, which indicates ground and tree squirrels have evolved to have more compact femora as femoral size increases. Chipmunk (-0.05 [-0.41:0.34]) and gliding squirrel (0.06 [-0.02:0.14]) femoral Cg was not significantly related with femoral centroid size. There were no significant differences in femoral Cg among ecotypes (PGLS with an ANCOVA design: R^2 = 0.27, λ = 0.00; femoral Cg [95% CI] for chipmunks = 0.14 [-0.07:0.35], gliding squirrels = 0.13 [-0.11:0.37], ground squirrels = 0.16 [-0.06:0.38], and tree squirrels = 0.11 [-0.11:0.35]; Fig. 6).

There was no significant relationship between femoral DE and femoral size across all ecotypes (PGLS: R^2 = 0.15, λ = 0.74, slope [95% CI] = -1.08 [-2.97:0.81]). Scaling relationships differed among ecotypes (PGLS with an ANCOVA design: R^2 = 0.58, λ = 0.00). Tree squirrel (-2.22 [-4.54:-0.02]) and ground squirrel (-2.41 [-4.38:-0.43]) femoral DE were significantly negatively related with femoral centroid size, indicating that tree and ground squirrels have evolved to have less elongate femora as femoral size increases. Chipmunk (-1.99 [-12.54:7.70]) and gliding squirrel (1.51 [-0.91:3.93]) femoral DE were not significantly related with femoral centroid size. There was a significant relationship between humeral DE and ecotype (PGLS with ANCOVA design: R^2 = 0.55, λ = 0.00) where gliding squirrels exhibited higher DE values (mean femoral DE [95% CI] = 32.50 [25.25:39.80]) and thus more elongate femoral diaphyses than ground squirrels (25.04 [18.24:31.71]) but not chipmunks (27.37 [21.25:33.27]) or tree squirrels (27.55 [20.60:34.38]; Fig. 6).

There was no significant relationship between femoral CSS and femoral size across all ecotypes (PGLS: $R^2 = 0.01$, $\lambda = 0.34$, slope [95% CI] = -0.08 [-0.23:0.06]) as well as within each ecotype (PGLS with an ANCOVA design: $R^2 = 0.42$, $\lambda = 0.00$; chipmunk femoral CSS = 0.59 [-0.42:1.59], gliding squirrel = -0.01 [-0.26:0.23], ground squirrel = -0.07 [-0.25:0.13], and tree squirrel = -0.09 [-0.31:0.10]). There were no significant differences in femoral CSS among ecotypes (mean femoral CSS [95% CI] for chipmunks = 1.80 [1.20:2.37], gliding squirrels = 1.55 [0.84:2.22], ground squirrels = 1.91 [1.25:2.52], and tree squirrels = 1.63 [0.97:2.25]; Fig. 6).

Comparisons between humeral and femoral internal structure

We found that global compactness (Cg) differed between the humerus and femur in chipmunks (humeral Cg = 0.60±0.05; femoral Cg =0.53±0.09; $p = 0.006$), ground squirrels (humeral Cg = 0.66±0.07; femoral Cg = 0.60±0.07; $p < 0.001$); and tree squirrels (humeral Cg = 0.61±0.08;femoral Cg = 0.56±0.08; $p < 0.001$). In contrast, Cg did not differ between the humerus (0.61±0.06) and femur (0.60±0.05) in gliding squirrels ($p = 0.610$).

Diaphysis elongation (DE) differed between the humerus and femur with each ecotype (chipmunks: humeral DE = 17.32±1.06, femoral DE = 21.05±1.25, $p < 0.001$; gliding squirrels: humeral DE = 22.39±2.14, femoral DE = 25.00±2.00, $p < 0.001$; ground squirrels: humeral DE = 14.81±1.66, femoral DE = 18.02±2.02, $p < 0.001$; tree squirrels: humeral DE = 16.92±1.47, femoral DE = 20.40±2.25, $p < 0.001$).

Lastly, cross-sectional shape (CSS) differed between the humerus and femur in only chipmunks (humeral CSS = 1.26±0.13, femoral CSS = 1.56±0.14, $p < 0.001$). There were no significant differences in CSS between the humerus and femur within the remaining ecotypes

383 (gliding squirrels: humeral CSS =1.26±0.11, femoral CSS = 1.27±0.12, p = 0.746; ground
384 squirrel: humeral CSS = 1.70±0.37, femoral CSS = 1.65±0.26, p = 0.490; tree squirrel: humeral
385 Cg = 1.45±0.20, femoral Cg = 1.36±0.12, p = 0.069).
386
387 *Relationships between external shape and internal structure*
388 In the humerus, the relationships between cross-sectional shape (CSS) and external shape
389 and diaphysis elongation (DE) and external shape were significant across squirrels (Table 2).
390 Furthermore, the interaction term between humeral CSS and ecotype was significant; however,
391 post-hoc pairwise tests revealed that relationships between humeral CSS and humeral external
392 shape did not differ among ecotypes. There was no relationship between humeral bone
393 compactness (Cg) and humeral external shape across and among ecotypes (Table 2).
394 In the femur, the relationship between DE and external shape was significant across
395 squirrels and among ecotypes (Table 2); however, post-hoc pairwise tests revealed that
396 relationships between femoral DE and femoral external shape did not differ among ecotypes.
397 Similarly, post-hoc pairwise tests revealed that relationships between femoral Cg and femoral
398 external shape did not differ among ecotypes despite the significant interaction term (Cg *
399 ecotype) in the full model (Table 2). There was no relationship between femoral CSS and
400 femoral external shape across and among ecotypes (Table 2).
401
402 **Discussion**
403 Size, locomotor ecology, and phylogenetic structure are often identified as the leading
404 factors that underlie limb bone variation in mammals (e.g., Fabre et al. 2013; Kilbourne and
405 Hoffman 2013; Martín-Serra et al. 2014b, 2014a; Mielke et al. 2018; Scheidt et al. 2019; Wölfer

et al. 2019; Etienne et al. 2021). Here, we found that these factors exhibit different relationships with the external shape and internal structures of squirrel humeri and femora: phylogenetic structure influenced variation of the external shape of these squirrel limb bones, whereas interactions between size and ecotype influenced variation of the internal structures.

Contrary to our prediction, the external shape of neither the humerus nor the femur exhibited significant allometry with respect to size when accounting for phylogeny (Fig. 3), and individual ecotypes also did not exhibit significant humeral or femoral shape allometry. These results indicate that there is no evolutionary transition from relatively elongate, gracile humeri and femora to relatively shorter, robust ones with increasing size in squirrels as found in other mammalian clades (Fabre et al. 2013; Martín-Serra et al. 2014a, 2014b; Etienne et al. 2021). These patterns are primarily influenced by the phylogenetic relationships among species as analyses without incorporating phylogenetic structure indicated femoral shape allometry that is primarily driven by gliding and ground squirrels (Supplementary Table S2). Similarly, we found a significant relationship between limb shape and ecotype without accounting for phylogeny where gliding squirrels tend to exhibit gracile, elongate humeri and femora; ground squirrels tend to exhibit robust humeri and femora; and chipmunks and tree squirrels tend to exhibit intermediate humeri and femora (Fig. 4; Table 1). However, these associations between ecotype and external shape of either the humerus or femur are lost when analyses account for phylogenetic relationships among species (Table 1). That accounting for phylogenetic relationships erased these relationships is not surprising considering squirrel ecotypes are phylogenetically clustered (Fig. 4); chipmunks and gliding squirrels are each monophyletic, ground squirrels consists of two clades, and tree squirrels are ancestral (Fig. 1). These results

428 suggest that the diversity of squirrel limb bones is partitioned early between clades rather than
429 between ecological groups.

430 In contrast, bone structure variables of the humerus and femur exhibited various
431 allometric trends. Across all squirrels, global compactness (Cg) of both the humerus and femur
432 increased with increasing limb size (Fig. 5), a pattern consistent with findings that cortical bone
433 thickness (Currey and Alexander 1985) and cross-sectional properties of the femur (Mielke et al.
434 2018; Scheidt et al. 2019) scale with increasing size. These positive relationships may be due to
435 the increase in mechanical stress at larger body sizes (McMahon 1973; Biewener 1990;
436 Christiansen 1999). In CSS, humeral cross-sections became more oval shaped as size increased,
437 but there was no significant relationship between femoral CSS and size. Lastly, we did not find
438 allometry in diaphysis elongation (DE) for both the humerus and femur across all squirrels.

439 Allometric patterns in bone structure variables are further nuanced by ecological
440 specialization. In ground squirrels, positive allometry of limb bone structures is consistent with
441 positive allometry of more robust body shapes (Linden et al. 2023), which together may serve as
442 adaptations for the digging and clearing stages of scratch digging during burrow construction.
443 The digging stage consists of the claws of the forelimbs striking the ground while the hind limbs
444 supports the body (Gasc et al. 1985; Hildebrand 1995), and a plethora of skeletal and muscular
445 adaptations in the forelimb are associated with this first stage (Lessa and Stein 1992; Hildebrand
446 1995; Lagaria and Youlatos 2006; Vassallo 2006; Steiner-Souza et al. 2010). Our finding of
447 positive allometry in humeral CSS provides additional evidence for adaptation towards digging,
448 particularly in larger ground squirrels with more oval cross sections that would increase the
449 muscle attachment sites needed for increased force production during digging. Positive allometry
450 of humeral Cg and trends towards positive allometry of humeral DE would also lead to more

451 compact, robust humeri that could decrease bone strain during the digging stage. These patterns
452 are also consistent with the phylomorphospace of humeral external shape. While there were no
453 significant differences in humeral external shape among ecotypes when accounting for
454 phylogeny, ground squirrel humeri occupied regions of phylomorphospace (+PC1) that are
455 associated with more pronounced deltoid tuberosities (Fig. 4A) that would provide greater
456 attachment surface area for deltoids and pectoral muscles, which are needed to increase the force
457 output advantageous for digging (Hildebrand 1985; Samuels and Van Valkenburgh 2008). These
458 humeri associated with +PC1 also exhibited more pronounced medial condyles that would
459 provide greater attachment sites for the extensor group key for scratch digging (Samuels and Van
460 Valkenburgh 2008; Steiner-Souza et al. 2010).

461 Unlike in the humerus, our results for the relationships between femoral morphology and
462 digging behavior are not as consistent. The clearing stage of scratch digging consists of the hind
463 limb removing excess soil through backward extension while the body is supported by the
464 forelimbs (Gasc et al. 1985; Hildebrand 1995). Whereas some have hypothesized that more
465 robust femora in fossorial species would improve stability and load transfer during clearing
466 (Casinos et al. 1993; Hildebrand 1995), others have hypothesized that fossorial species exhibit
467 less robust femora to reflect less rigidity in bending and torsion compared to species that jump or
468 run with their hind limbs (Gambaryan 1974; Biknevicius 1993; Wölfer et al. 2019). Furthermore,
469 some have also hypothesized that robust femora are not a necessary adaptation because the hind
470 limbs are only used to shovel away excess substrate during the clearing stage that had previously
471 been loosened with the forelimbs during the digging stage (Gambaryan 1974; Wölfer et al.
472 2019). Our findings support both these hypotheses: positive allometry of femoral Cg and
473 negative allometry of DE indicates that ground squirrel femora evolved to be more compact and

474 robust with increasing femoral size, which may decrease bone deformation during the clearing
475 phase. Conversely, the lack of allometry in femoral CSS suggests that the femur is less
476 specialized for digging compared to the humerus. Ground squirrel femora occupied regions of
477 phylomorphospace (+PC1) (Fig. 4B) that are associated with more pronounced greater
478 trochanters. These adaptations reflect the larger muscle attachment area for the gluteal muscles,
479 which when enlarged in fossorial species may help the body resist being pushed back when
480 digging, respectively (Samuels and Van Valkenburgh 2008).

481 In tree squirrels, humeri and femora exhibited greater Cg with increasing bone size.
482 Additionally, we found that tree squirrels evolved more robust diaphyses (i.e., lower DE) in both
483 humeri and femora as bone size increases. This contrasts with prior findings that scansorial or
484 arboreal mammals often exhibit more elongate limb bones as size increases to increase limb span
485 (Polly 2007; Kilbourne and Hoffman 2013). However, this may be due to the somewhat unique
486 climbing method employed by tree squirrels, which use their claws to interlock into tree bark and
487 their muscle strength to hold their bodies close to the tree as they climb (Schmidt and Fischer
488 2011). At larger body sizes, tree squirrels may need to counter the additional body weight by
489 remaining relatively closer to the tree to minimize opposing forces. No significant relationships
490 were observed between either humeral or femoral CSS and bone size in tree squirrels. This may
491 point to a more generalized cross-sectional shape being satisfactory for climbing behavior across
492 different sizes.

493 No significant bone structure allometry was observed in neither chipmunks nor gliders.
494 The lack of allometry in chipmunks may be due to their small sizes and limited size range. Prior
495 research in other small mammals have shown that the ability of bone tissue to remodel in
496 response to its mechanical environment (i.e., Wolff's Law) may be restricted by body size

(Dawson 1980; Meier et al. 2013). This makes specialization of bone structure traits such as compactness less likely to occur, as overall humeral morphology may be sufficient for digging or climbing without further cortical adaptations. Another explanation is that chipmunks primarily dig shallow shelters instead of extensive burrow systems and thus may not require extreme shape specializations (Samuels and Van Valkenburgh 2008). That chipmunk humeri and femora share overlapping regions of phylomorphospace with both tree and ground squirrels (Fig. 4) support these hypotheses. The lack of allometry in gliding squirrels may be due to wing loading (body mass / patagium area); larger gliding squirrels decrease the detrimental effects of higher wing loading by exhibiting a lower relative body weight instead of evolving relatively longer limbs compared to smaller gliding squirrels (Thorington and Heaney 1981). Nevertheless, gliding squirrels on average exhibited more elongate humeri and femora compared to other ecotypes (Fig. 4; Fig. 6), consistent with previous findings (Peterka 1936; Bryant 1945; Thorington and Heaney 1981; Grossnickle et al. 2020; Linden et al. 2023).

Comparing humeral and femoral structure

Previous studies suggest that scansorial mammals exhibit similar global compactness values between the forelimb and the hindlimb due to the equal importance of both limbs during climbing, whereas scratch-digging mammals exhibit higher compactness in the forelimb due to the many specializations associated with digging (Hildebrand 1985; Straehl et al. 2013). We found higher mean global compactness in humeri than in femora in chipmunks and ground squirrels, an expected result since chipmunks and ground squirrels exhibit forelimb specializations associated with a fossorial lifestyle (Lessa and Stein 1992; Hildebrand 1995; Lagaria and Youlatos 2006; Vassallo 2006; Steiner-Souza et al. 2010). Surprisingly, tree

520 squirrels also exhibited higher mean global compactness in humeri than in femora. A possible
521 explanation is that although tree squirrels are scansorial, they are not limited to only climbing.
522 Tree squirrels are often found running on the forest floor, and often bury food by scratch-digging
523 (Ferron 1981). This may help to explain some of the adaptions seen in tree squirrels that have
524 been historically correlated with fossorial locomotion. We also found higher DE values in the
525 femur compared to the humerus in each of the four ecotypes. More elongate femora support
526 previous findings that rodent humeri tend to be the shortest long bone whereas rodent femora are
527 typically one of the longest (Prodinger et al. 2018). Lastly, only chipmunks exhibited higher CSS
528 values in the femur compared to the humerus, with the femora being more ovular-shaped at the
529 midshaft cross-section while the humeri were more circular-shaped.
530
531 **Conclusion**
532 We found that size, locomotor ecology, and underlying phylogenetic structure exhibited
533 different relationships with the external shape and internal structure of squirrel humeri and
534 femora. Although humeral and femoral shape can be predicted by ecotype, all squirrel ecotypes
535 are largely phylogenetically clustered and accounting for phylogenetic relationships among
536 species removes these associations. These results suggest that the diversity of squirrel limb bones
537 is partitioned early between clades rather than between ecological groups. Clade-based
538 evolutionary shifts in morphologies have been found in other mammals such as carnivorans
539 (Law 2021; Law et al. 2022). Whether humeral and femoral shape variation evolved in relation
540 to different ecologies early in squirrel evolutionary history and subsequently maintained within
541 clades remains to be investigated. In contrast, interactions between size and ecotype influenced
542 variation of the internal structures after accounting for phylogenetic relationships. The humeri

and femora of ground and tree squirrels tended to exhibit increased bone compactness and more robust diaphyses with increasing bone size, and only ground squirrel humeri exhibited more oval-shaped cross-sections with increasing humeral size. Overall, these results indicate that mechanical and phylogenetic constraints and ecology may enact different pressures on the external and internal parts of the limb bones. Increasing the number of species across the squirrel phylogeny and expanding to other rodents will enable us to tease apart the effects of selection and phylogeny on potentially converging limb morphologies. Together, this work provides a strong morphological foundation for future research investigating the evolutionary biomechanics and ecology of squirrel locomotion.

Funding

J.R. was supported by a National Science Foundation Postdoctoral Research Fellowship REU Program; A.E.B. was supported by the American Museum of Natural History REU program, the Mary Gates Endowment, and the American Society of Mammalogists Grant-in-Aid of Research Award; T.J.L. was supported by the American Museum of Natural History REU program and the John and Dorothy Franco Charitable Foundation; S.E.S. was supported by the National Science Foundation [IOS-2017738]; and C.J.L. was supported by the National Science Foundation [DBI-1906248, DBI–2128146], the Gerstner Family Foundation and the Richard Gilder Graduate School at the American Museum of Natural History, an Iuvo Postdoctoral Award at the University of Washington, and a University of Texas Early Career Provost Fellowship.

Acknowledgements

The authors are grateful to the collections and its staff of the Burke Museum of Natural History, California Academy of Sciences, Florida Museum of Natural History, Museum of Vertebrate Zoology, Natural History Museum of Los Angeles County, Slater Museum of Natural History, Smithsonian Institute Natural Museum of Natural History, University of Kansas Biodiversity Institute & Natural History Museum, and Yale Peabody Museum. We thank Jonathan Huie for helpful suggestions on using SegmentGeometry, Kelly Diamond for helpful suggestions on using SlicerMorph, Jack Tseng and Dave Grossnickle for CT scanning some specimens, and the staff of Friday Harbor Labs for allowing us to CT scan specimens.

Data Availability Statement

The data underlying this article are available in the Dryad Digital Repository, at https://dx.doi.org/[XXXXX]

Figures

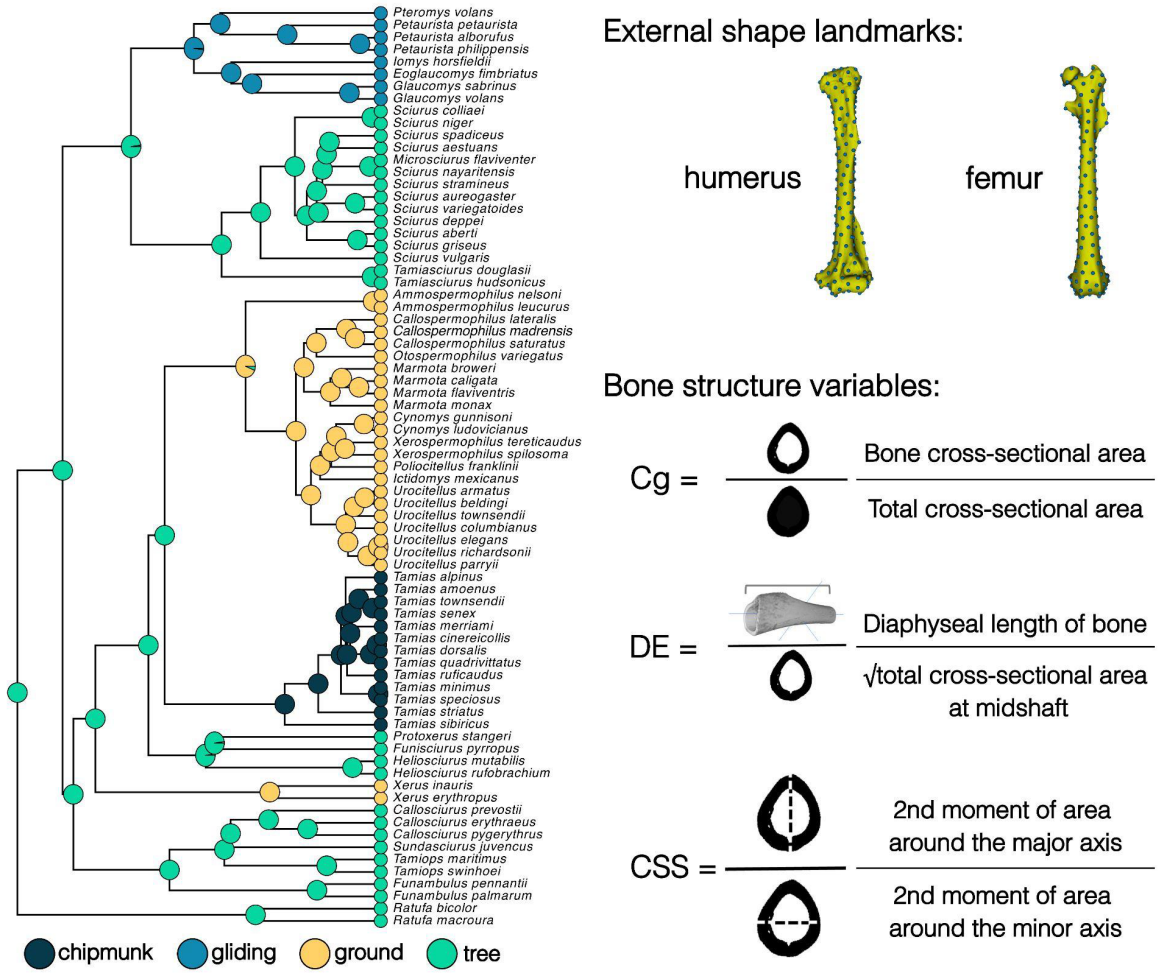

585

586 Fig. 1. Overview of the species and morphometrics used. The pruned phylogeny is overlaid with
587 an ancestral state reconstruction of squirrel ecotype. 194 pseudolandmarks on the humeri and
588 152 pseudolandmarks on the femora were generated and applied to our sample using the
589 PseudoLMGenerator (Rolfe et al. 2021) and ALPACA modules (Porto et al. 2021) in
590 SlicerMorph. Bone structure variables were calculated using the SegmentGeometry module
591 (Huie et al. 2022) in Slicer. Cg = global compactness; DE = diaphysis elongation; CSS = cross-
592 sectional shape.

593

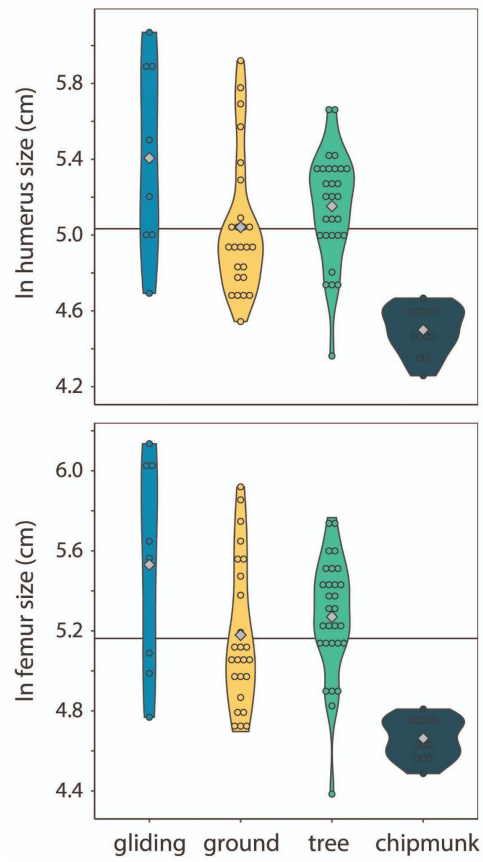

Fig. 2. Violin plots of ln humeral size and ln femoral size by ecotype. Chipmunks exhibited significantly smaller humeri and femora compared to gliding and tree squirrels but not ground squirrels. The horizontal black line indicates the mean size across all ecotypes.

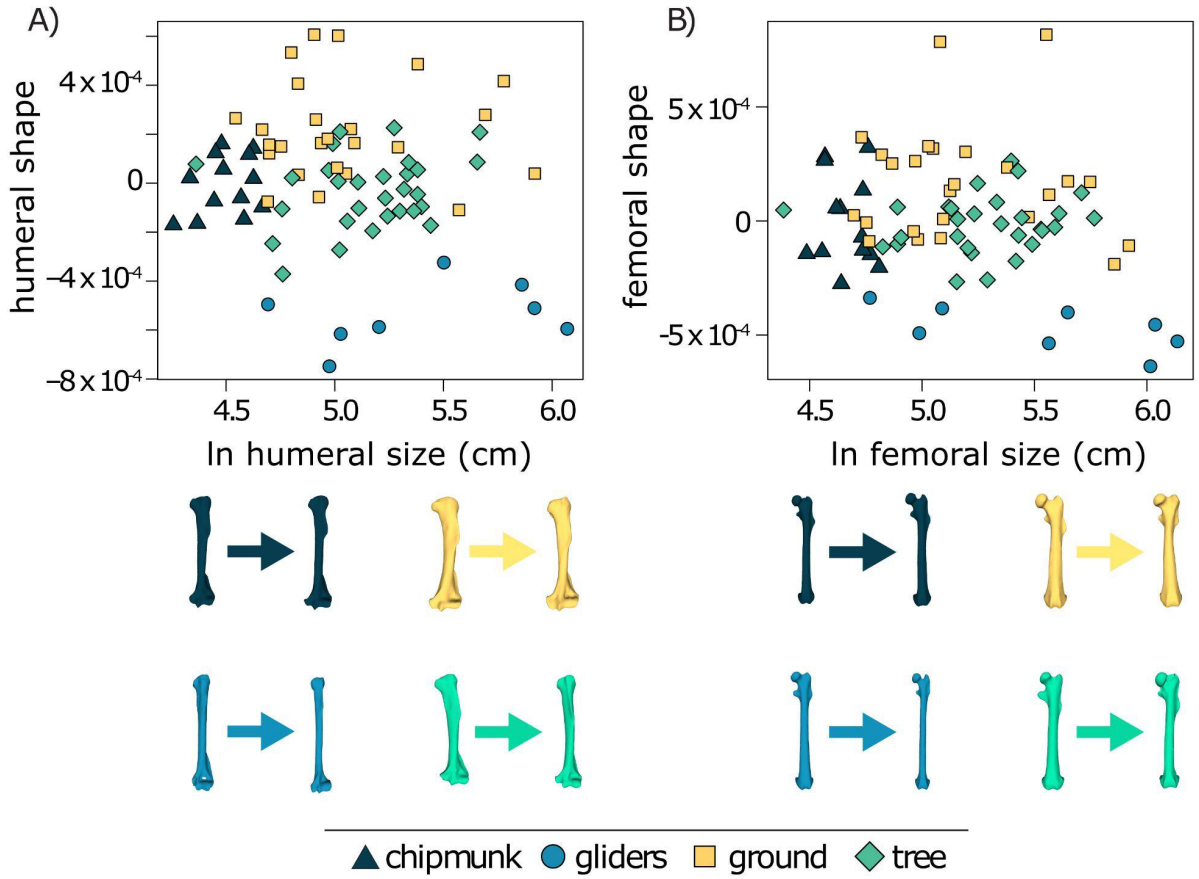

Fig. 3. Allometric trends between external shape and size of the A) humerus and B) femur. Limb bone images show the difference in shape from the smallest to biggest species in each ecotype (chipmunk: *Tamias alpinus* to *Tamias townsendii*; gliding: *Glaucomys volans* to *Petaurista petaurista*; ground: *Callospermophilus madrensis* to *Marmota caligata*; tree: *Tamiops maritimus* to *Ratufa macroura*).

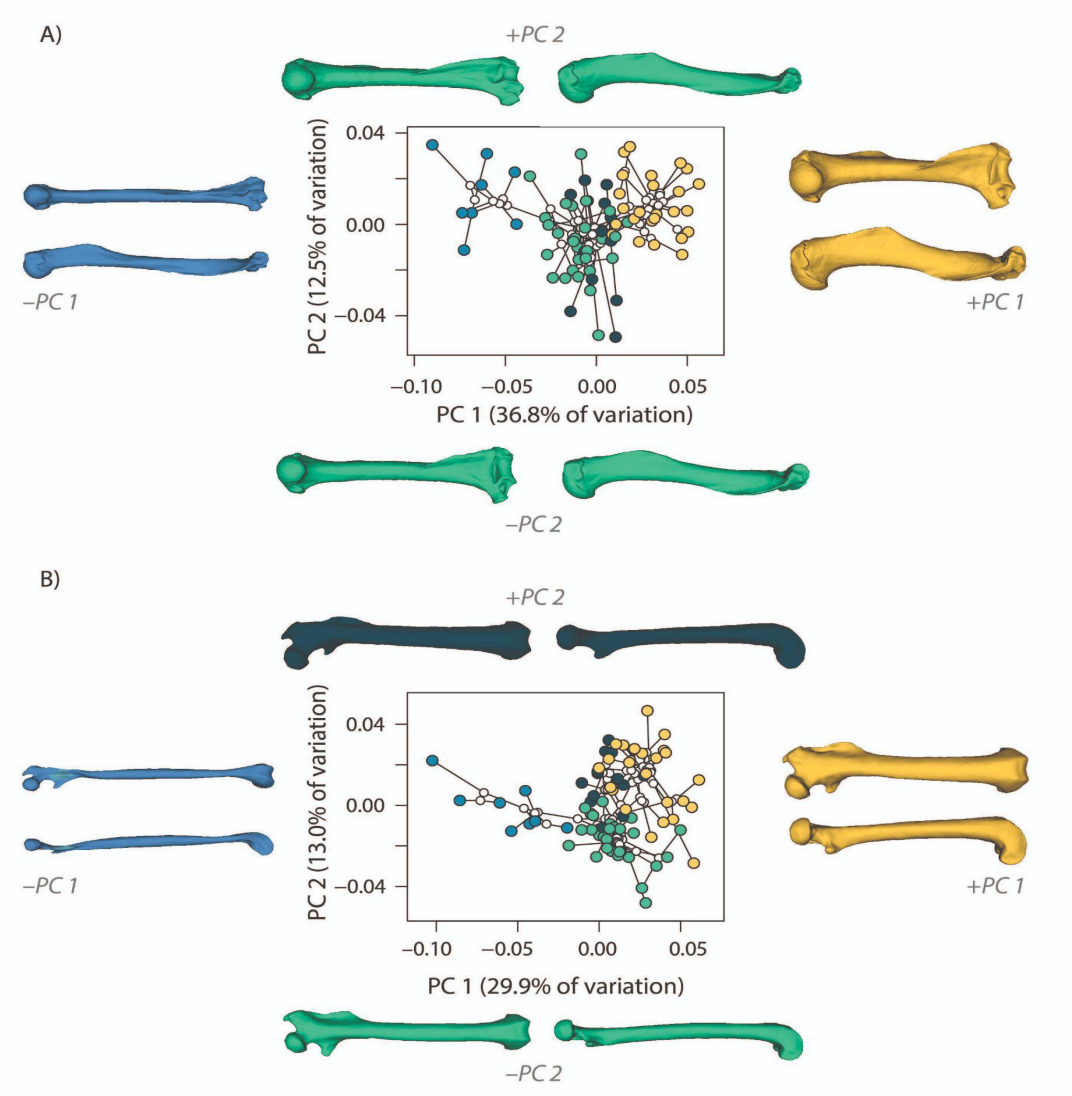

Fig. 4. Phylomorphospaces of A) humeral shape and B) femoral shape with PC1-2 extremes for visualization. The humeral and femoral models reflect the computationally determined PC1 and 2 extremes, and their colors reflect the ecotype associated with extreme ends of the first two PCs. Blue circles represent gliding squirrels, yellow circles represent ground squirrels, navy circles represent chipmunks, green circles represent tree squirrels, and open circles represent tree nodes within the phylomorphospace.

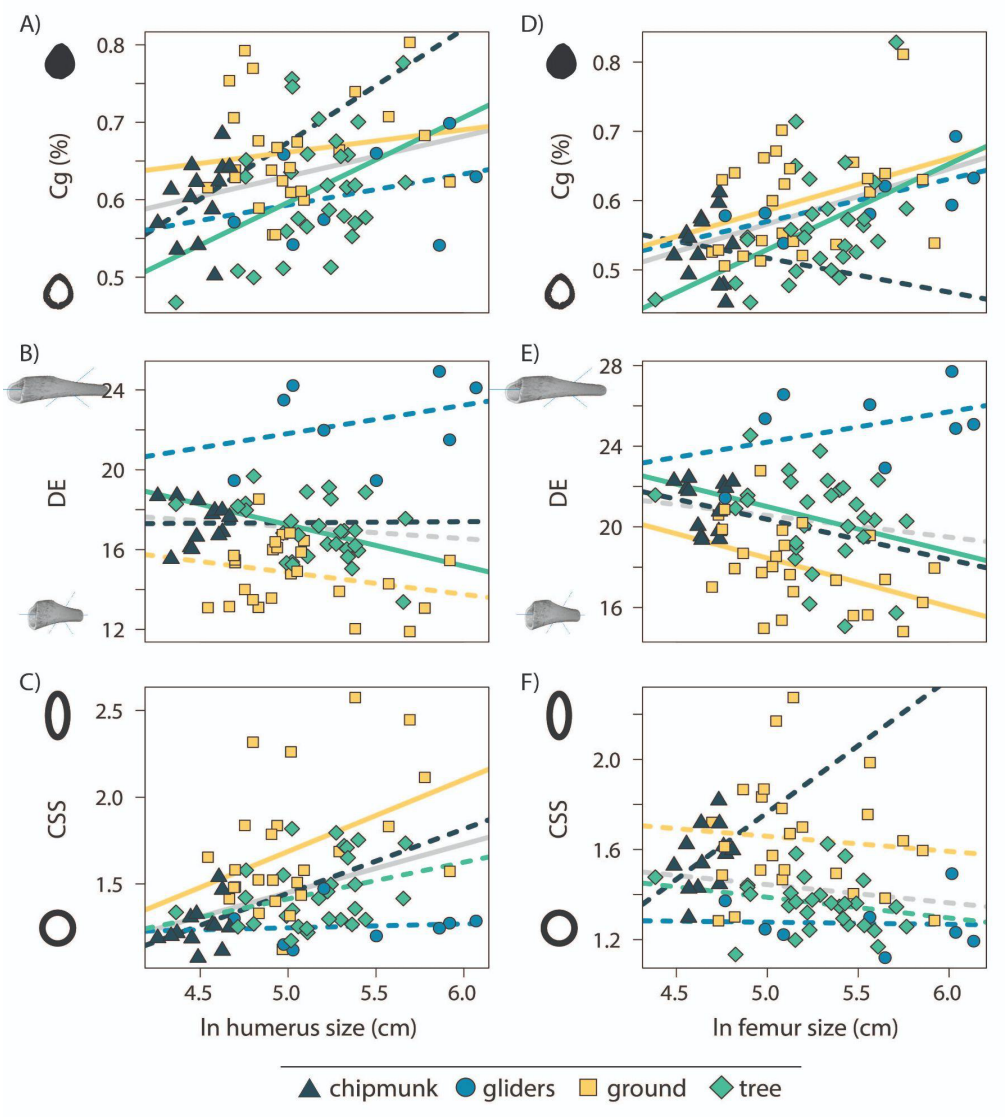

614

615 Fig. 5. Scatter plot of ln limb size and each bone structure variable in the humerus (A-C) and

616 femur (D-F). Confidence intervals that deviated from an isometric slope of 0 were interpreted as

617 exhibiting significant positive allometry (slope > 0) or negative allometry (slope < 0). Solid lines

618 depict significant allometry, whereas dashed lines depict no significant allometry. Gray lines

619 indicate relationships across all squirrel ecotypes. Cg = global compactness; DE = diaphysis

620 elongation; cross-sectional shape = CSS.

621

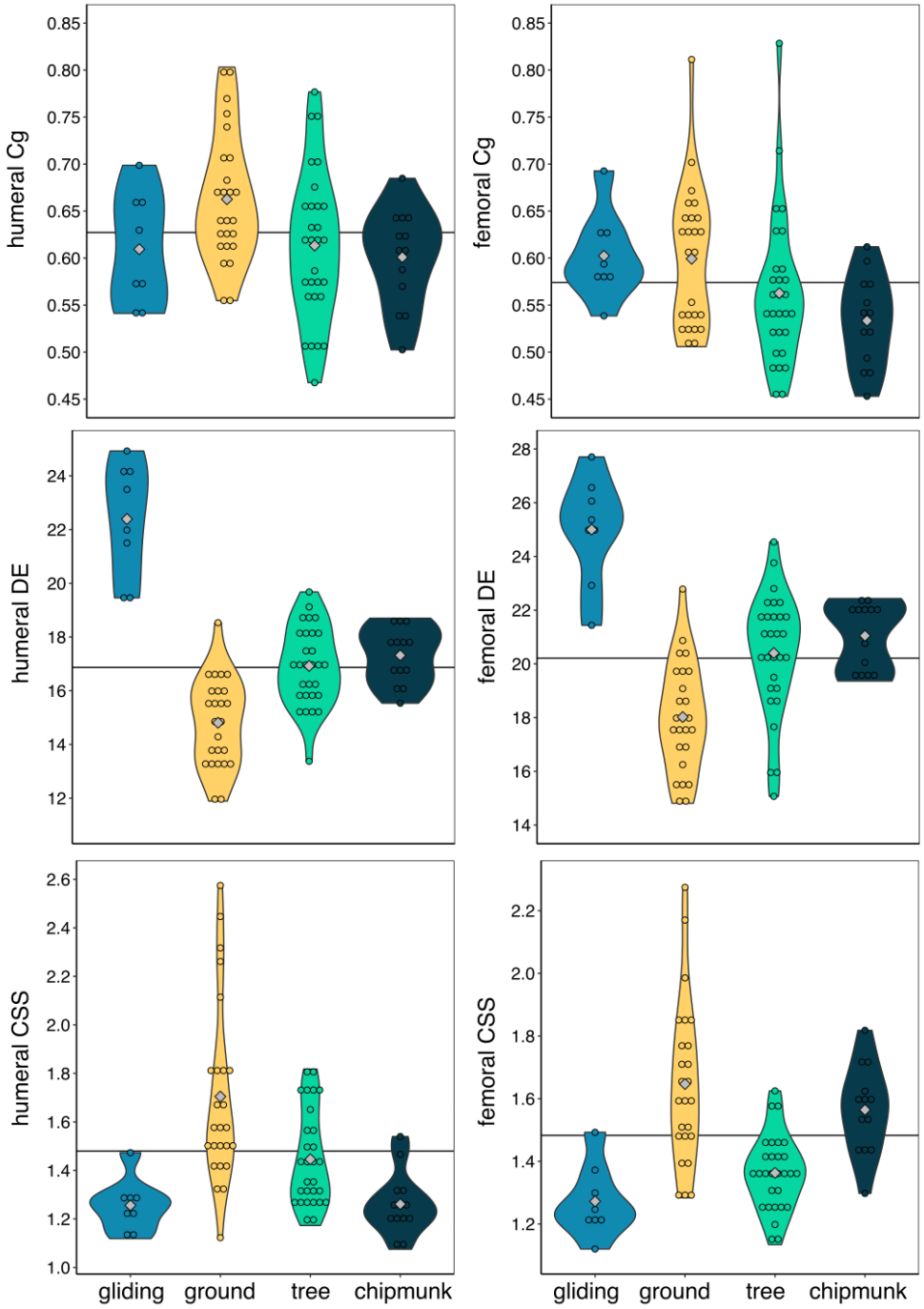

Fig. 6. Violin plots of raw bone structure variables in humeri and femora. Variables are not corrected for allometry. Cg = global compactness; DE = diaphysis elongation; cross-sectional shape = CSS.

Table 1. Results of the Procrustes ANCOVA and phylogenetic Procrustes ANCOVA with random residual permutation procedure (RRPP) for humeral shape and femoral shape. Bolded P values indicate significance (alpha = 0.05). DF, degrees of freedom; SS, sum of squares.

	Procrustes ANCOVA						phylogenetic Procrustes ANCOVA					
Humeral shape	DF	SS	R2	F	Z	P	DF	SS	R2	F	Z	P
ln humeral size	1	0.002	0.01	1.34	0.95	0.179	1	0.002	0.02	1.46	1.11	0.127
ecotype	3	0.072	0.37	14.32	6.55	**0.001**	3	0.003	0.04	1.05	-0.14	0.550
ln humeral size * ecotype	3	0.007	0.04	1.40	1.68	0.050	3	0.006	0.07	1.67	1.37	0.089
Residuals	67	0.113	0.57				67	0.074	0.88			
Total	74	0.198					74	0.084				
Femoral shape	DF	SS	R2	F	Z	P	DF	SS	R2	F	Z	P
ln femoral size	1	0.003	0.01	1.61	1.63	0.056	1	0.001	0.01	0.88	0.23	0.409
ecotype	3	0.063	0.29	10.40	6.79	**0.001**	3	0.003	0.04	0.95	-0.36	0.649
ln femoral size * ecotype	3	0.013	0.06	2.15	3.45	**0.001**	3	0.007	0.08	1.94	1.73	0.050
Residuals	67	0.136	0.61				67	0.080	0.88			
Total	74	0.222					74	0.091				

Table 2. Results of phylogenetic Procrustes ANCOVA with random residual permutation procedure (RRPP) for relationships between external shape and each internal bone structure variable among ecotypes. Bolded P values indicate significance (alpha = 0.05). DF, degrees of freedom; SS, sum of squares.

Humerus	DF	SS	R^2	F	Z	P
Cg	1	0.003	0.03	2.517	1.609	0.052
ecotype	3	0.003	0.04	1.051	-0.121	0.549
Cg * ecotype	3	0.006	0.07	1.871	1.588	0.064
Residuals	67	0.072	0.86			
Total	74	0.084				
DE	1	0.006	0.07	5.385	3.372	**0.001**
ecotype	3	0.003	0.04	1.014	-0.188	0.584
DE * ecotype	3	0.005	0.06	1.517	1.434	0.077
Residuals	67	0.070	0.84			
Total	74	0.084				
CSS	1	0.003	0.03	2.478	1.966	**0.020**
ecotype	3	0.003	0.04	1.063	-0.127	0.547
CSS * ecotype	3	0.009	0.10	2.729	2.215	**0.014**
Residuals	67	0.070	0.83			
Total	74	0.084				

Femur	DF	SS	R^2	F	Z	P
Cg	1	0.002	0.02	1.941	1.449	0.077
ecotype	3	0.003	0.04	0.982	-0.289	0.603
Cg * ecotype	3	0.007	0.08	2.126	1.929	**0.038**
Residuals	67	0.078	0.86			
Total	74	0.091				
DE	1	0.006	0.07	5.910	3.992	**0.001**
ecotype	3	0.003	0.04	1.020	-0.221	0.593
DE * ecotype	3	0.008	0.09	2.362	2.382	**0.008**
Residuals	67	0.073	0.81			
Total	74	0.091				
CSS	1	0.002	0.02	1.588	1.311	0.105
ecotype	3	0.003	0.04	0.938	-0.392	0.648
CSS * ecotype	3	0.006	0.07	1.834	1.235	0.109
Residuals	67	0.079	0.87			
Total	74	0.091				

References

Adams D, Collyer M, Kaliontzopoulou A, Baken E. 2022. Geomorph: Software for geometric morphometric analyses. .

Adams DC, Collyer ML. 2018. Multivariate Phylogenetic Comparative Methods: Evaluations, Comparisons, and Recommendations. Syst Biol 67:14–31.

Alexander RMcN, Jayes AS, Maloiy GMO, Wathuta EM. 1979. Allometry of the limb bones of mammals from shrews (Sorex) to elephant (Loxodonta). J Zool 189:305–14.

Amson E, Bibi F. 2021. Differing effects of size and lifestyle on bone structure in mammals. BMC Biol 19:87.

Amson E, Billet G, de Muizon C. 2018. Evolutionary adaptation to aquatic lifestyle in extinct sloths can lead to systemic alteration of bone structure. Proc R Soc B Biol Sci 285:20180270.

Amson E, Scheyer TM, Martinez Q, Schwermann AH, Koyabu D, He K, Ziegler R. 2022. Unique bone microanatomy reveals ancestry of subterranean specializations in mammals. Evol Lett 6:552–61.

Baken EK, Collyer ML, Kaliontzopoulou A, Adams DC. 2021. geomorph v4.0 and gmShiny: Enhanced analytics and a new graphical interface for a comprehensive morphometric experience. Methods Ecol Evol 12:2355–63.

Biewener AA. 1983. Allometry of Quadrupedal Locomotion: the Scaling of Duty Factor, Bonecurvature and Limb Orientation to Body Size. J Exp Biol 105:147–71.

Biewener AA. 1990. Biomechanics of Mammalian Terrestrial Locomotion. Science 250:1097–1103.

Biknevicius AR. 1993. Biomechanical Scaling of Limb Bones and Differential Limb Use in

667 Caviomorph Rodents. J Mammal 74:95–107.
668 Bryant MD. 1945. Phylogeny of Nearctic Sciuridae. Am Midl Nat 33:257.
669 Burr DB, Ruff CB, Johnson C. 1989. Structural adaptations of the femur and humerus to arboreal
670 and terrestrial environments in three species of macaque. Am J Phys Anthropol 79:357–
671 67.
672 Campione NE, Evans DC. 2012. A universal scaling relationship between body mass and
673 proximal limb bone dimensions in quadrupedal terrestrial tetrapods. BMC Biol 10:60.
674 Casinos A, Quintana C, Viladiu C. 1993. Allometry and adaptation in the long bones of a
675 digging group of rodents (Ctenomyinae). Zool J Linn Soc 107:107–15.
676 Christiansen P. 1999. Scaling of the limb long bones to body mass in terrestrial mammals. J
677 Morphol 239:167–90.
678 Clavel J, Aristide L, Morlon H. 2019. A Penalized Likelihood Framework for High-Dimensional
679 Phylogenetic Comparative Methods and an Application to New-World Monkeys Brain
680 Evolution. Syst Biol 68:93–116.
681 Clavel J, Escarguel G, Merceron G. 2015. mvmorph: an r package for fitting multivariate
682 evolutionary models to morphometric data. Methods Ecol Evol 6:1311–19.
683 Clavel J, Morlon H. 2020. Reliable Phylogenetic Regressions for Multivariate Comparative
684 Data: Illustration with the MANOVA and Application to the Effect of Diet on Mandible
685 Morphology in Phyllostomid Bats. Syst Biol 69:927–43.
686 Collyer ML, Sekora DJ, Adams DC. 2015. A method for analysis of phenotypic change for
687 phenotypes described by high-dimensional data. Heredity 115:357–65.
688 Cowin SC, Sadegh AM, Luo GM. 1992. An Evolutionary Wolff's Law for Trabecular
689 Architecture. J Biomech Eng 114:129–36.

690 Currey JD, Alexander RMcN. 1985. The thickness of the walls of tubular bones. J Zool
691 206:453–68.
692 Dawson DL. 1980. Functional interpretations of the radiographic anatomy of the femora of
693 Myotis iucifugus, Pipistrellus subflavus, and Blarina brevicauda. Am J Anat 157:1–15.
694 Demes B, Jungers WL. 1993. Long bone cross-sectional dimensions, locomotor adaptations and
695 body size in prosimian primates. J Hum Evol 25:57–74.
696 Diamond KM, Burtner AE, Siddiqui D, Alvarado K, Leake SL, Rolfe S, Zhang C, Kwon RY,
697 Maga AM. 2022. Examining craniofacial variation among crispant and mutant zebrafish
698 models of human skeletal diseases. .
699 Doube M, Conroy AW, Christiansen P, Hutchinson JR, Shefelbine S. 2009. Three-Dimensional
700 Geometric Analysis of Felid Limb Bone Allometry. PLOS ONE 4:e4742.
701 Etienne C, Filippo A, Cornette R, Houssaye A. 2021. Effect of mass and habitat on the shape of
702 limb long bones: A morpho-functional investigation on Bovidae (Mammalia:
703 Cetartiodactyla). J Anat 238:886–904.
704 Fabre A-C, Cornette R, Goswami A, Peigné S. 2015. Do constraints associated with the
705 locomotor habitat drive the evolution of forelimb shape? A case study in musteloid
706 carnivorans. J Anat 226:596–610.
707 Fabre A-C, Cornette R, Peigné S, Goswami A. 2013. Influence of body mass on the shape of
708 forelimb in musteloid carnivorans. Biol J Linn Soc 110:91–103.
709 Fedorov A, Beichel R, Kalpathy-Cramer J, Finet J, Fillion-Robin J-C, Pujol S, Bauer C, Jennings
710 D, Fennessy F, Sonka M, Buatti J, Aylward S, Miller JV, Pieper S, Kikinis R. 2012. 3D
711 Slicer as an image computing platform for the Quantitative Imaging Network. Magn
712 Reson Imaging, Quantitative Imaging in Cancer 30:1323–41.

Ferron J. 1981. Comparative Ontogeny of Behaviour in Four Species of Squirrels (Sciuridae). Z Für Tierpsychol 55:193–216.

Gambaryan PP. 1974. How Mammals Run: Anatomical Adaptations Wiley.

Gasc J-P, Renous S, Casinos A, Laville E, Bou J. 1985. Comparison of diverse digging patterns in some small mammals. Fortschr Zool 30:35–38.

Grossnickle DM, Chen M, Wauer JGA, Pevsner SK, Weaver LN, Meng Q-J, Liu D, Zhang Y-G, Luo Z-X. 2020. Incomplete convergence of gliding mammal skeletons*. Evolution 74:2662–80.

Hayssen V. 2008. Patterns of Body and Tail Length and Body Mass in Sciuridae. In: Journal of Mammalogy p. 852–73.

Hildebrand M. 1985. Chapter 6. Digging of Quadrupeds. In: Hildebrand M, Bramble DM, Liem KF, Wake DB, editors. Functional Vertebrate Morphology Harvard University Press. p. 89–109.

Hildebrand M. 1995. Analysis of vertebrate structure. 4th ed. ed New York: J. Wiley.

Huie JM, Summers AP, Kawano SM. 2022. SegmentGeometry: A Tool for Measuring Second Moment of Area in 3D Slicer. Integr Org Biol 4:obac009.

Hunt NH, Jinn J, Jacobs LF, Full RJ. 2021. Acrobatic squirrels learn to leap and land on tree branches without falling. Science 373:697–700.

Kikinis R, Pieper SD, Vosburgh KG. 2014. 3D Slicer: A Platform for Subject-Specific Image Analysis, Visualization, and Clinical Support. In: Jolesz FA, editor. Intraoperative Imaging and Image-Guided Therapy New York, NY: Springer. p. 277–89.

Kilbourne BM, Hoffman LC. 2013. Scale Effects between Body Size and Limb Design in Quadrupedal Mammals. PLOS ONE 8:e78392.

Kimura T. 1991. Long and robust bones of primates. In: Ehara A, editor. Primatology Today: Proceedings of the XIIIth Congress of the International Primatological Society, Nagoya and Kyoto, 18-24, July 1990 Amsterdam; New York: Elsevier Science Publishers.

Kivell TL. 2016. A review of trabecular bone functional adaptation: what have we learned from trabecular analyses in extant hominoids and what can we apply to fossils? J Anat 228:569–94.

Lagaria A, Youlatos D. 2006. Anatomical Correlates to Scratch Digging in the Forelimb of European Ground Squirrels (Spermophilus citellus). J Mammal 87:563–70.

Law CJ. 2021. Ecological Drivers of Carnivoran Body Shape Evolution. Am Nat 198:406–20.

Law CJ, Blackwell EA, Curtis AA, Dickinson E, Hartstone-Rose A, Santana SE. 2022. Decoupled evolution of the cranium and mandible in carnivoran mammals. Evolution 76:2959–74.

Lessa EP, Stein BR. 1992. Morphological constraints in the digging apparatus of pocket gophers (Mammalia: Geomyidae). Biol J Linn Soc 47:439–53.

Linden T, Burtner A, Rickman J, McFeely A, Santana S, Law C. 2023. Scaling patterns of body plans differ among squirrel ecotypes. PeerJ 11:e14800.

Martín-Serra A, Figueirido B, Palmqvist P. 2014a. A Three-Dimensional Analysis of Morphological Evolution and Locomotor Performance of the Carnivoran Forelimb. PloS One 9:e85574.

Martín-Serra A, Figueirido B, Palmqvist P. 2014b. A three-dimensional analysis of the morphological evolution and locomotor behaviour of the carnivoran hind limb. BMC Evol Biol 14:129.

McMahon T. 1973. Size and shape in biology. Science 179:1201–4.

759 Meier PS, Bickelmann C, Scheyer TM, Koyabu D, Sánchez-Villagra MR. 2013. Evolution of
760 bone compactness in extant and extinct moles (Talpidae): exploring humeral
761 microstructure in small fossorial mammals. BMC Evol Biol 13:55.
762 Mielke M, Wölfer J, Arnold P, van Heteren AH, Amson E, Nyakatura JA. 2018. Trabecular
763 architecture in the sciuromorph femoral head: allometry and functional adaptation. Zool
764 Lett 4:10.
765 Montoya-Sanhueza G, Chinsamy A. 2017. Long bone histology of the subterranean rodent
766 Bathyergus suillus (Bathyergidae): ontogenetic pattern of cortical bone thickening. J Anat
767 230:203–33.
768 Peterka HE. 1936. A Study of the Myology and Osteology of Tree Sciurids with Regard to
769 Adaptation to Arboreal, Glissant and Fossorial Habits. Trans Kans Acad Sci 1903-
770 39:313–32.
771 Polly PD. 2007. Limbs in Mammalian Evolution. In: Hall KB, editor. Fins into Limbs:
772 Evolution, Development, and Transformation Chicago: University of Chicago Press. p.
773 245–68.
774 Porto A, Rolfe S, Maga AM. 2021. ALPACA: A fast and accurate computer vision approach for
775 automated landmarking of three-dimensional biological structures. Methods Ecol Evol
776 12:2129–44.
777 Prodinger PM, Foehr P, Bürklein D, Bissinger O, Pilge H, Kreutzer K, von Eisenhart-Rothe R,
778 Tischer T. 2018. Whole bone testing in small animals: systematic characterization of the
779 mechanical properties of different rodent bones available for rat fracture models. Eur J
780 Med Res 23:8.
781 Rohlf FJ, Slice D. 1990. Extensions of the Procrustes Method for the Optimal Superimposition

782 of Landmarks. Syst Biol 39:40–59.
783 Rolfe S, Pieper S, Porto A, Diamond K, Winchester J, Shan S, Kirveslahti H, Boyer D, Summers
784 A, Maga AM. 2021. SlicerMorph: An open and extensible platform to retrieve, visualize
785 and analyse 3D morphology. Methods Ecol Evol 12:1816–25.
786 Ruff C, Holt B, Trinkaus E. 2006. Who's afraid of the big bad Wolff?: "Wolff's law" and bone
787 functional adaptation. Am J Phys Anthropol 129:484–98.
788 Ryan TM, Shaw CN. 2013. Trabecular bone microstructure scales allometrically in the primate
789 humerus and femur. Proc R Soc B Biol Sci 280:20130172.
790 Samuels JX, Van Valkenburgh B. 2008. Skeletal indicators of locomotor adaptations in living
791 and extinct rodents. J Morphol 269:1387–1411.
792 Schaffler MB, Burr DB, Jungers WL, Ruff CB. 1985. Structural and Mechanical Indicators of
793 Limb Specialization in Primates. Folia Primatol (Basel) 45:61–75.
794 Scheidt A, Wölfer J, Nyakatura JA. 2019. The evolution of femoral cross-sectional properties in
795 sciuromorph rodents: Influence of body mass and locomotor ecology. J Morphol
796 280:1156–69.
797 Schlager S. 2017. Chapter 9 - Morpho and Rvcg – Shape Analysis in R: R-Packages for
798 Geometric Morphometrics, Shape Analysis and Surface Manipulations. In: Zheng G, Li
799 S, Székely G, editors. Statistical Shape and Deformation Analysis Academic Press. p.
800 217–56.
801 Schmidt A, Fischer MS. 2011. The kinematic consequences of locomotion on sloped arboreal
802 substrates in a generalized (Rattus norvegicus) and a specialized (Sciurus vulgaris)
803 rodent. J Exp Biol 214:2544–59.
804 Steiner-Souza F, De Freitas TRO, Cordeiro-Estrela P. 2010. Inferring adaptation within shape

diversity of the humerus of subterranean rodent Ctenomys. Biol J Linn Soc 100:353–67.

Straehl FR, Scheyer TM, Forasiepi AM, MacPhee RD, Sánchez-Villagra MR. 2013. Evolutionary Patterns of Bone Histology and Bone Compactness in Xenarthran Mammal Long Bones. PLOS ONE 8:e69275.

Thorington RW Jr, Heaney LR. 1981. Body Proportions and Gliding Adaptations of Flying Squirrels (Petauristinae). J Mammal 62:101–14.

Tung Ho L si, Ané C. 2014. A Linear-Time Algorithm for Gaussian and Non-Gaussian Trait Evolution Models. Syst Biol 63:397–408.

Upham NS, Esselstyn JA, Jetz W. 2019. Inferring the mammal tree: Species-level sets of phylogenies for questions in ecology, evolution, and conservation. PLOS Biol 17:e3000494.

Vassallo A. 2006. Functional morphology, comparative behaviour, and adaptation in two sympatric subterranean rodents genus Ctenomys (Caviomorpha: Octodontidae). J Zool 244:415–27.

Wölfer J, Amson E, Arnold P, Botton-Divet L, Fabre A-C, van Heteren AH, Nyakatura JA. 2019. Femoral morphology of sciuromorph rodents in light of scaling and locomotor ecology. J Anat 234:731–47.

Zelditch ML, Swiderski DL, Sheets HD. 2012. Chapter 1 - Introduction. In: Zelditch ML, Swiderski DL, Sheets HD, editors. Geometric Morphometrics for Biologists (Second Edition) San Diego: Academic Press. p. 1–20.

826 **Supplementary Material**

827 Table S1. Museum specimens used in this study. CAS = California Academy of Sciences; KU =
828 University of Kansas Biodiversity Institute & Natural History Museum; LACM = Natural
829 History Museum of Los Angeles County; MVZ = UC Berkeley Museum of Vertebrate Zoology;
830 PSM = University of Puget Sound Slater Museum of Natural History; UF = Florida Museum of
831 Natural History; USNM = Smithsonian National Museum of Natural History; UWBM =
832 University of Washington Burke Museum of Natural History

species	catalog number	ecotype
Ammospermophilus leucurus	UWBM74646	ground
Ammospermophilus nelsoni	MVZ234368	ground
Callosciurus erythraeus	CAS6371	tree
Callosciurus prevostii	LACM97346	tree
Callosciurus pygerythrus	PSM27419	tree
Callospermophilus lateralis	UWBM38960	ground
Callospermophilus madrensis	MVZ99799	ground
Callospermophilus saturatus	UWBM38984	ground
Cynomys gunnisoni	MVZ99763	ground
Cynomys ludovicianus	UWBM75774	ground
Eoglaucomys fimbriatus	USNM173363	gliding
Funambulus palmarum	MVZ183704	tree
Funambulus pennantii	UF30290	tree
Funisciurus pyrropus	MVZ196233	tree
Glaucomys sabrinus	UWBM35058	gliding
Glaucomys volans	UWBM43897	gliding
Heliosciurus mutabilis	MVZ220919	tree
Heliosciurus rufobrachium	MVZ196227	tree
Ictidomys mexicanus	MVZ93789	ground
Iomys horsfieldii	PSM10370	gliding
Marmota broweri	UWBM82831	ground
Marmota caligata	UWBM31095	ground
Marmota flaviventris	UWBM32500	ground
Marmota monax	UWBM39792	ground
Microsciurus flaviventer	MVZ154935	tree
Otospermophilus variegatus	UWBM79876	ground
Petaurista alborufus	MVZ183717	gliding

Petaurista petaurista	USNM197320	gliding
Petaurista philippensis	USNM314973	gliding
Poliocitellus franklinii	UWBM33260	ground
Protoxerus stangeri	MVZ196230	tree
Pteromys volans	UWBM39689	gliding
Ratufa bicolor	MVZ123699	tree
Ratufa macroura	UWBM21183	tree
Sciurus aberti	UWBM35277	tree
Sciurus aestuans	MVZ182070	tree
Sciurus aureogaster	LACM053653	tree
Sciurus colliaei	LACM058790	tree
Sciurus deppei	MVZ98319	tree
Sciurus griseus	UWBM76257	tree
Sciurus nayaritensis	UWBM81981	tree
Sciurus niger	UWBM35230	tree
Sciurus spadiceus	MVZ166023	tree
Sciurus stramineus	MVZ135638	tree
Sciurus variegatoides	MVZ131091	tree
Sciurus vulgaris	UWBM39069	tree
Sundasciurus juvencus	KU165382	tree
Tamias alpinus	MVZ207209	chipmunk
Tamias amoenus	UWBM31698	chipmunk
Tamias cinereicollis	UWBM38257	chipmunk
Tamias dorsalis	UWBM78908	chipmunk
Tamias merriami	UWBM60172	chipmunk
Tamias minimus	UWBM30813	chipmunk
Tamias quadrivittatus	UWBM35301	chipmunk
Tamias ruficaudus	UWBM34354	chipmunk
Tamias senex	UWBM78783	chipmunk
Tamias sibiricus	UWBM39259	chipmunk
Tamias speciosus	UWBM43059	chipmunk
Tamias striatus	UWBM35246	chipmunk
Tamias townsendii	UWBM35213	chipmunk
Tamiasciurus douglasii	UWBM81947	tree
Tamiasciurus hudsonicus	UWBM81510	tree
Tamiops maritimus	MVZ186481	tree
Tamiops swinhoei	UWBM75283	tree
Urocitellus armatus	MVZ64641	ground
Urocitellus beldingi	UWBM42459	ground
Urocitellus columbianus	UWBM74770	ground

Urocitellus elegans	UWBM33286	ground
Urocitellus parryii	UWBM39268	ground
Urocitellus richardsonii	UWBM32960	ground
Urocitellus townsendii	UWBM78333	ground
Xerospermophilus spilosoma	UWBM35284	ground
Xerospermophilus tereticaudus	UWBM35502	ground
Xerus erythropus	MVZ115437	ground
Xerus inauris	MVZ117287	ground

Table S2. Results of the Procrustes regressions and phylogenetic Procrustes regressions with random residual permutation procedure (RRPP) for humeral shape and femoral shape allometry within each ecotype. Bolded P values indicate significance (alpha = 0.05). DF, degrees of freedom; SS, sum of squares.

	Procrustes regression							phylogenetic Procrustes regression					
Humeral shape	DF	SS	R2	F	Z	P		DF	SS	R2	F	Z	P
chipmunks													
ln humeral size	1	0.002	0.08	1.00	0.24	0.406		1	0.016	0.17	2.17	0.84	0.217
Residuals	11	0.019	0.92					11	0.079	0.84			
Total	12	0.021						12	0.094				
gliding squirrels													
ln humeral size	1	0.003	0.30	2.57	2.30	**0.004**		1	0.007	0.25	1.97	0.88	0.21
Residuals	6	0.007	0.70					6	0.022	0.75			
Total	7	0.009						7	0.030				
ground squirrels													
ln humeral size	1	0.003	0.07	1.68	1.61	0.052		1	0.001	0.01	0.31	###	0.893
Residuals	23	0.045	0.93					23	0.040	0.99			
Total	24	0.048						24	0.041				
tree squirrels													
ln humeral size	1	0.002	0.03	0.95	0.08	0.470		1	0.001	0.03	0.81	0.33	0.374
Residuals	27	0.043	0.97					27	0.043	0.97			
Total	28	0.044						28	0.045				
	Procrustes regression							phylogenetic Procrustes regression					
Femoral shape	DF	SS	R2	F	Z	P		DF	SS	R2	F	Z	P
chipmunks													
ln humeral size	1	0.001	0.04	0.51	###	0.926		1	0.018	0.19	2.64	0.93	0.188
Residuals	11	0.020	0.96					11	0.077	0.81			
Total	12	0.021						12	0.095				
gliding squirrels													
ln humeral size	1	0.007	0.41	4.13	2.35	**0.004**		1	0.006	0.19	1.39	0.69	0.265
Residuals	6	0.010	0.59					6	0.025	0.81			
Total	7	0.017						7	0.031				
ground squirrels													
ln humeral size	1	0.006	0.09	2.21	2.27	**0.012**		1	0.001	0.02	0.46	###	0.765
Residuals	23	0.060	0.91					23	0.045	0.98			
Total	24	0.065						24	0.046				
tree squirrels													
ln humeral size	1	0.003	0.06	1.63	1.39	0.078		1	0.001	0.03	0.79	0.23	0.443
Residuals	27	0.046	0.94					27	0.043	0.97			
Total	28	0.049						28	0.044				